JUN JAEGYU* VOLCANO: A RECENTLY DISCOVERED ALKALI BASALT VOLCANO IN ANTARCTIC SOUND, ANTARCTICA

PETROGRAPHY, GEOCHEMISTRY, AND IMPLICATIONS FOR PETROGENESIS

By
Ashley K. Hatfield

An Independent Study in Petrology

Hamilton College
Clinton, NY
April 2005

JUN JAEGYU*

* The volcano is named in honor of Jun Jaegyu, a young Korean scientist who lost his life during the 2003 field season in the South Shetland Islands. He was participating in the Korean Antarctic Program through King Sejong Station.

ABSTRACT

Jun Jaegyu volcano is a young alkali basalt volcanic construct recently discovered by scientists aboard the NSF research vessel Laurence M. Gould in May 2004 (LMG04-04). The volcano lies on the Antarctic continental shelf in Antarctic Sound, north of the previously mapped boundary of Cenozoic volcanic rocks in the Antarctic Peninsula. Reports by mariners of discolored water in this region of Antarctic Sound, thermal anomalies associated with the volcano, as well as fresh volcanic rock dredged from the construct provide evidence suggesting recent volcanic activity. Petrographic analysis of selected samples reveal that olivine, clinopyroxene and plagioclase are present as phenocryst phases.

Major, trace, and rare earth element geochemical trends are consistent with those of other alkali basalt volcanoes analyzed from the Antarctic Peninsula region. These alkali basalt volcanoes show the strongest geochemical affinity to within-plate alkali basalts, such as OIB and CAB. However, the relative depletion of Ba and Rb in Antarctic Peninsula alkali basalts as compared to OIB and CAB causes many researchers to doubt the presence of a mantle plume under the Antarctic Peninsula. The use of $^{3}He/^{4}He$ isotopes as a petrogenetic indicator for a primordial mantle source component may provide valuable insight into the depth of the asthenospheric source region for Antarctic Peninsula alkali basalts.

TABLE OF CONTENTS

TABLE OF FIGURES

ACKNOWLEDGEMENTS

I wish to thank my advisor, Professor Dave Bailey, for the opportunity to study this volcano, as well as for all his guidance and encouragement on this project. Further, this project could not have been accomplished without the tireless efforts of Professor Eugene Domack, and I am grateful to him for providing me the opportunity to travel to the Antarctic. I also wish to acknowledge the scientists, officers and crew of the LMG04-04 during the 2004 Antarctic field season. Specifically, S. Brachfeld, Department of Earth and Environment Studies at Montclair State University in Upper Montclair, NJ; R. Gilbert, Department of Geological Sciences, Queen's University, Kingston, ON; S. Ishman, Department of Geology, Southern Illinois University, Carbondale, IL; G. Krahmann, Lamont-Doherty Earth Observatory, Palisades, NY; and A. Laventer, Department of Geology, Colgate University, Hamilton, NY.

Finally, the discovery of this volcano would not have been possible without the support provided by the U.S. National Science Foundation Office of Polar Programs.

CHAPTER 1

Introduction

The Antarctic plate constitutes one of the great alkaline volcanic regions of the world because the continent is internally broken by numerous large rift structures producing a nearly plate-wide extensional tectonic regime (LeMasurier, 1990). Cenozoic alkali basalts are widespread throughout West Antarctica at locations such as Marie Byrd Land, Ross Island, and the Antarctic Peninsula (Figure 1) (Hole, Smellie, and Marriner).

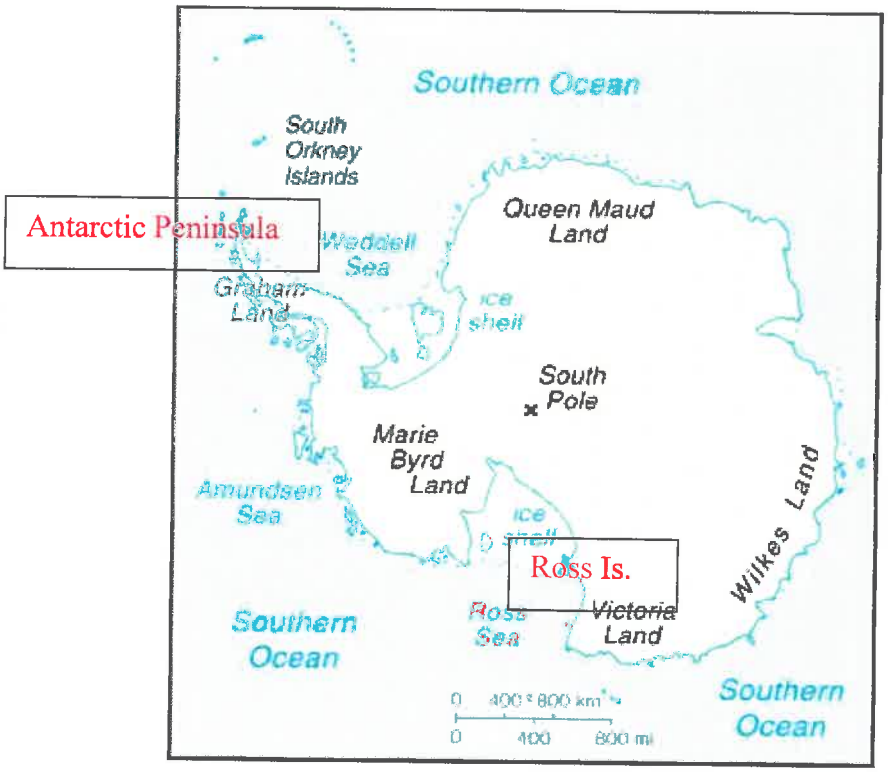

Figure 1: West Antarctica: Cenozoic Volcanism. Major alkalic basalt provinces of west Antarctica include the Antarctic Peninsula, Marie Byrd Land, and Ross Island (http://images.google.com/imgres?imgurl=http://www.exportinfo.org/worldfactbook/maps/antarctica_map.gif&imgrefurl=http://www.exportinfo.org/worldfactbook/antarctica_WFB.html&h=377&w=351&sz=35&tbnid=zXdWYYlxkvMJ:&tbnh=118&tbnw=110&hl=en&start=19&prev=/images%3F)

Further, many volcanoes likely remain undiscovered due to harsh climate conditions not conducive to exploration and research in the Antarctic (LeMasurier, 1990). The Antarctic Peninsula differs from the rest of the Cenozoic alkalic province due to its close temporal and spatial relationship with the cessation of subduction along the west coast (Hole, 1990). The discovery of Jun Jaegyu volcano in May 2004 by scientists aboard the

research vessel L.M. Gould (LMG04-04) increases the number of recognized alkali basalt volcanoes in the Antarctic Peninsula (Hatfield et. al., 2004).

The Antarctic Peninsula is characterized by the subduction of Pacific oceanic crust beneath the west coast for 200 Ma (Hole, 1988; Hole, 1990). The cessation of subduction was not uniform; rather, it proceeded step-wise progressively northwards between 50 Ma and 4 Ma (Smellie, 1987). Subduction completely ceased ~4 Ma through these northward-younging ridge crest-trench collisions (Hole, 1988; Hole, 1990). However, the Miocene-Recent volcanism of the Antarctic Peninsula, both in front of and behind the extinct calc-alkaline arc, is completely lacking in any of the distinctive geochemical and isotopic characteristics associated with the subduction of oceanic crust beneath a continental margin (Hole, 1990; Hole and Larter, 1993). Instead, following the cessation of subduction, the character of volcanism in the Antarctic Peninsula changed from calc-alkaline to alkaline (Hole, 1988; Hole, 1990).

Within-plate alkaline basaltic rocks occur scattered along the whole length of the Antarctic Peninsula and postdate the cessation of subduction between 6 and 40 Ma (Hole, 1990; Hole and Larter, 1993; Hole and LeMasurier, 1994; Smellie, 1987). The major occurrences of post-subduction within-plate basalts include Alexander Island, James Ross Island, and the Seal Nunataks (Hole, 1990). Jun Jaegyu Volcano lies north of these three volcanic centers, in Antarctic Sound (Figure 2) (Hatfield et. al., 2004). At Alexander Island, following the cessation of subduction, a Miocene-Pliocene suite of basanites, tephrites, and alkali and olivine basalts erupted 15 to < 1 Ma (Hole, 1988; Hole and Larter, 1993). The Seal Nunataks consist of alkali and olivine basalts and minor volumes of within-plate tholeiites erupted < 4 Ma (Hole, 1990; Hole and Larter, 1993). The

geochemical similarities of the post-subduction basalts erupted along the Antarctic Peninsula imply the existence of a chemically similar asthenospheric source region (Hole and Larter, 1993).

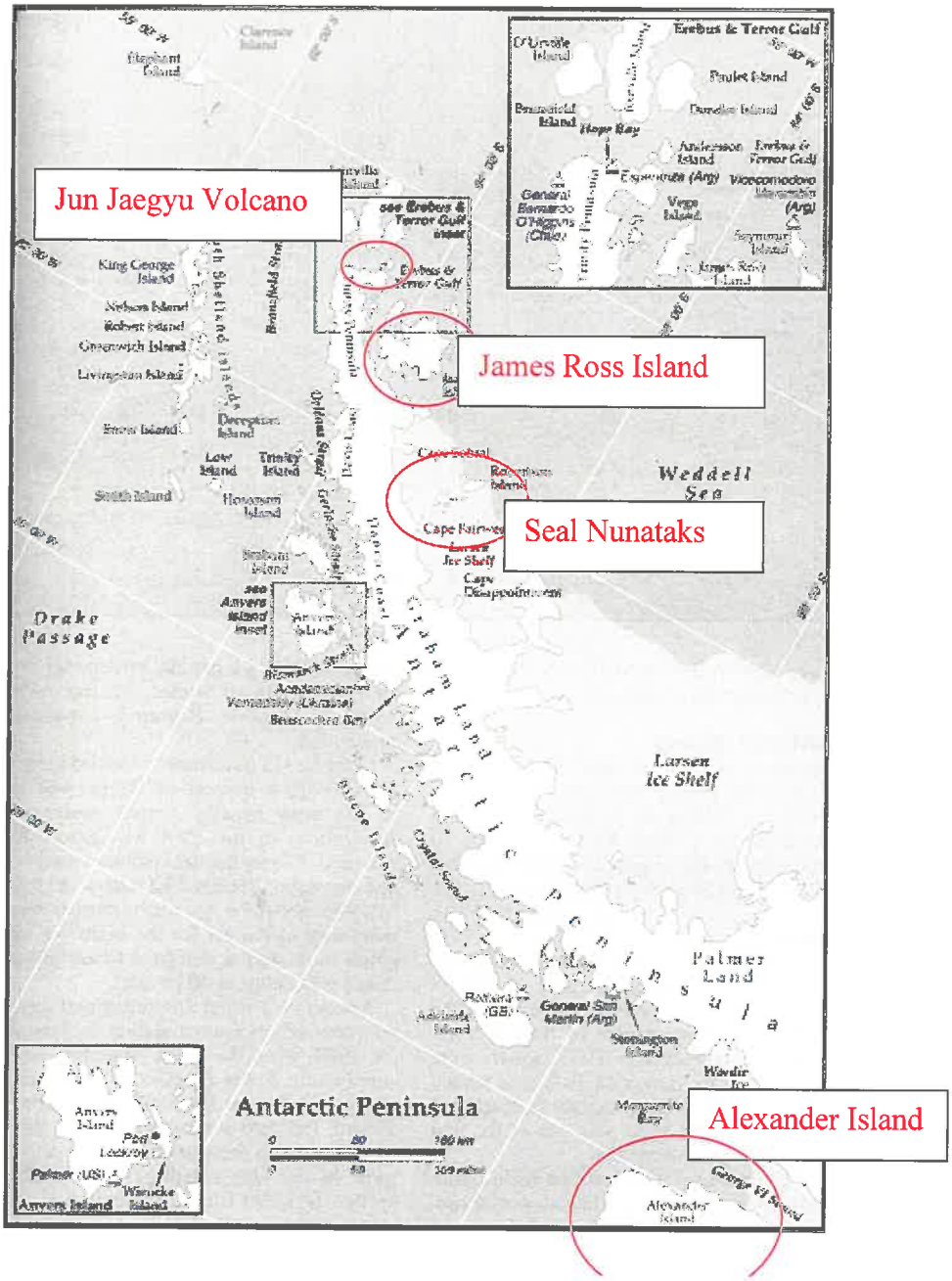

Figure 2: Antarctic Peninsula: Within-plate Alkali Basalts. Three major occurrences of post-subduction within-plate alkali basalts include Alexander Island, the Seal Nunataks and James Ross Island. Jun Jaegyu Volcano lies north of these three locations, in Antarctic Sound (http://www.heritage-antarctica.org/ahtuk/images/peninsula1.gif).

Post-subduction high-Mg andesites related to the cessation of subduction at other continental margins are absent on the Antarctic Peninsula, most likely because of the specific plate configurations of the Antarctic Peninsula (Hole, 1990). Instead, the basalts have incompatible trace element and isotopic variations broadly consistent with those of continental alkali basalts and OIB (Hole, 1988; Hole and Larter, 1993; Hole and LeMasurier, 1994). It is considered that continental alkali basalts and OIB depth of generation is deep: up to 650 km (Hole, 1988). However, unlike continental alkali basalts and OIB, it is thought that the alkaline volcanism in the Antarctic Peninsula cannot be related to mantle plume activity (Smellie, 1987).

Hole et al., 1990, proposed a "no-slab window" petrogenetic model for the generation of the within-plate alkalic basalts of the Antarctic Peninsula (Hole and Larter, 1993; Hole and LeMasurier, 1994). A "no-slab window" is a subducted slab-free region beneath the continental crust that formed during the late Cenozoic following the ridge crest-trench collisions (Hole and Larter, 1993; Hole and LeMasurier, 1994). The upwelling of asthenosphere into the voids left open by the continued sinking of the leading plate following collision resulted in decompressional melting (Hole and Larter, 1993). In this model, the spontaneous formation of a mantle plume is not necessary to explain the production of alkalic magmas (Hole and LeMasurier, 1994).

Tectonic Setting

The Antarctic plate is almost completely encircled by mid-ocean ridges along approximately 95% of its perimeter (LeMasurier, 1990). The plate has been stationary for possibly as long as the past 80 Ma (Hole and LeMasurier, 1994). Currently, the Antarctic Peninsula region exhibits extension, subduction, and transform boundaries

Goal of this Study

The goal of this study is to investigate and characterize the petrography, geochemistry and petrogenesis of Jun Jaegyu volcano. Specifically, we wish to determine 1) whether Jun Jaegyu retains a remnant geochemical subduction signature, and 2) the depth of generation for the Jun Jaegyu alkali basalts. Assuming that the alkali basalt volcanoes of the Antarctic Peninsula have a common asthenospheric source region, the information obtained from Jun Jaegyu may apply to the other volcanoes scattered throughout the Antarctic Peninsula region.

CHAPTER 2

Discovery of Jun Jaegyu

Scientists aboard the NSF Antarctic research vessel Laurence M. Gould (LMG04-04) discovered Jun Jaegyu Volcano in May 2004. The volcano lies in southern Antarctic Sound, northwest of Rosamel Island and 9 km due north of the easternmost point of Andersson Island, approximately 63 29 (°S), 56 26 (°W) (LMG04-04, Cruise Report; Hatfield et al., 2004). The existence of this volcano, as well as three other volcanoes in the surrounding region, was suspected based on a swath bathymetry map compiled from a research cruise in 2001 (NBP01-07) (Figure 4). In 2004, on-station data collection included a swath bathymetry map, a scud (submarine camera underwater device) equipped with a pressure thermister gauge, and a rock dredge (LMG04-04, Cruise Report; Hatfield et al., 2004).

Swath bathymetry data gathered by a Seabeam Multibeam Echosounder revealed an elongate, symmetrical construct that stands approximately 700 meters above the seafloor and extends to within approximately 275 meters of the ocean surface. The seamount contains approximately 1.5 km^3 of volcanic rock. The volcano truncates a glacially carved channel within Antarctic Sound and lies adjacent to a northwest-southeast oriented fault scarp. Furthermore, the volcano lies north of the mapped boundary of Late Cenozoic volcanic rocks (Figure 4) (Hatfield et al., 2004).

Figure 4: Swath Bathymetry Map of Antarctic Sound (Hatfield et al., 2004).

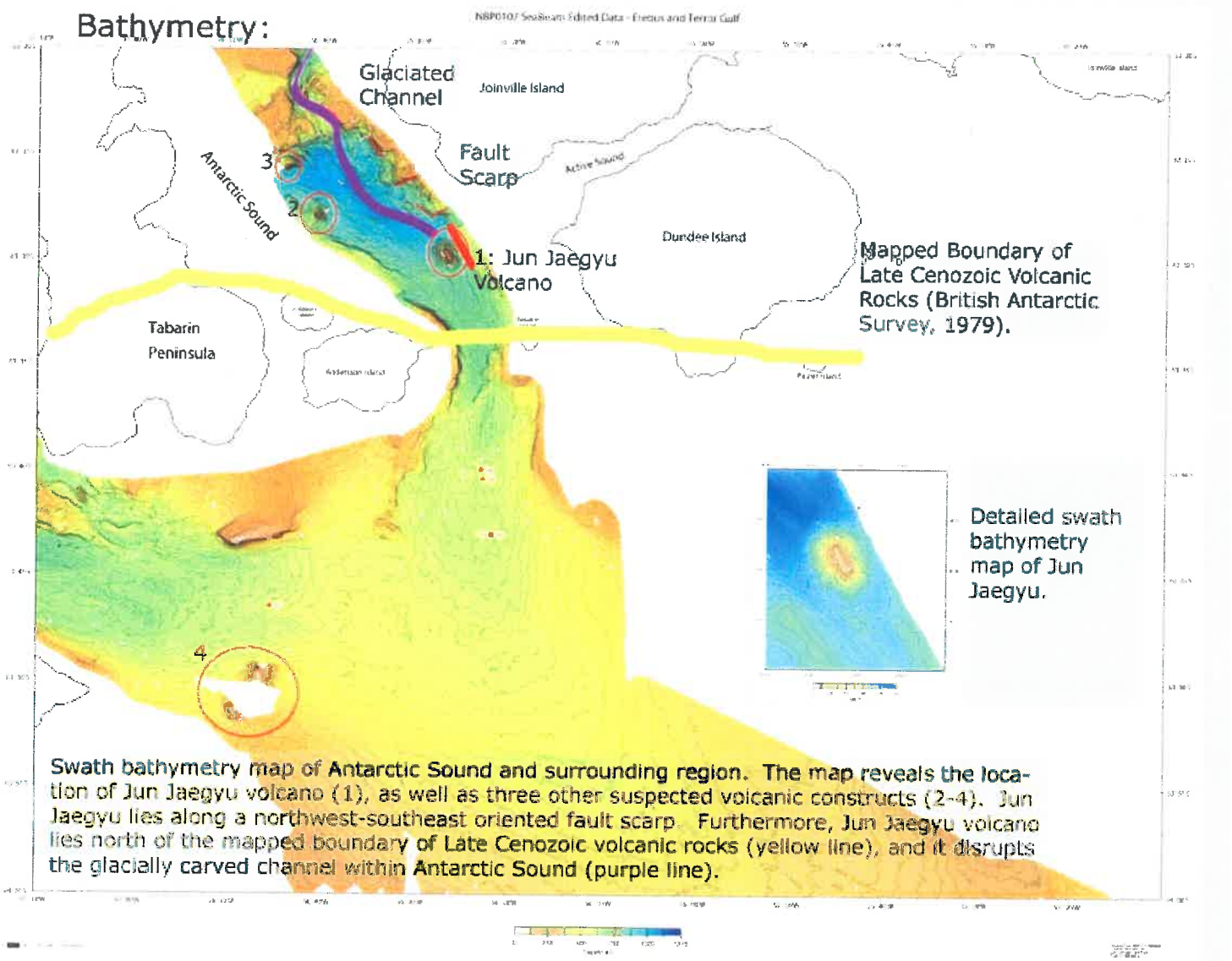

The scud traversed the surface of the volcano along a south to north route recording video footage and thermal anomalies along its path (Figure 5) (Hatfield et al., 2004). A graph plotting temperature against time reveals a southern and a northern temperature anomaly (Figure 6) (Hatfield et al., 2004). These irregularities suggest the possibility that two volcanic centers may exist. The more complex northern temperature anomaly correlates to fresher basalt flows as viewed on the video footage.

Figure 5: Scud Traverse (Hatfield et al., 2004)

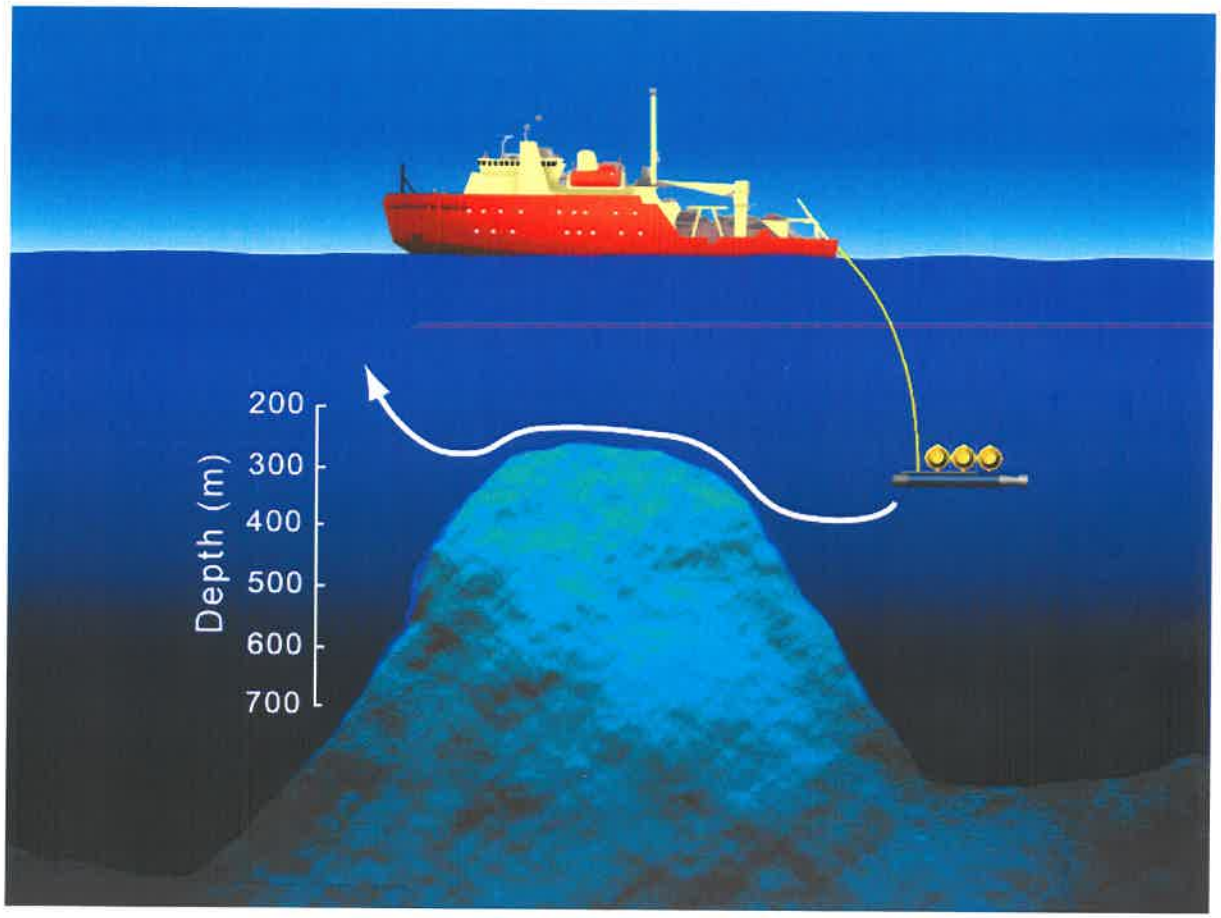

Figure 6: Thermal Anomalies (Hatfield et al., 2004)

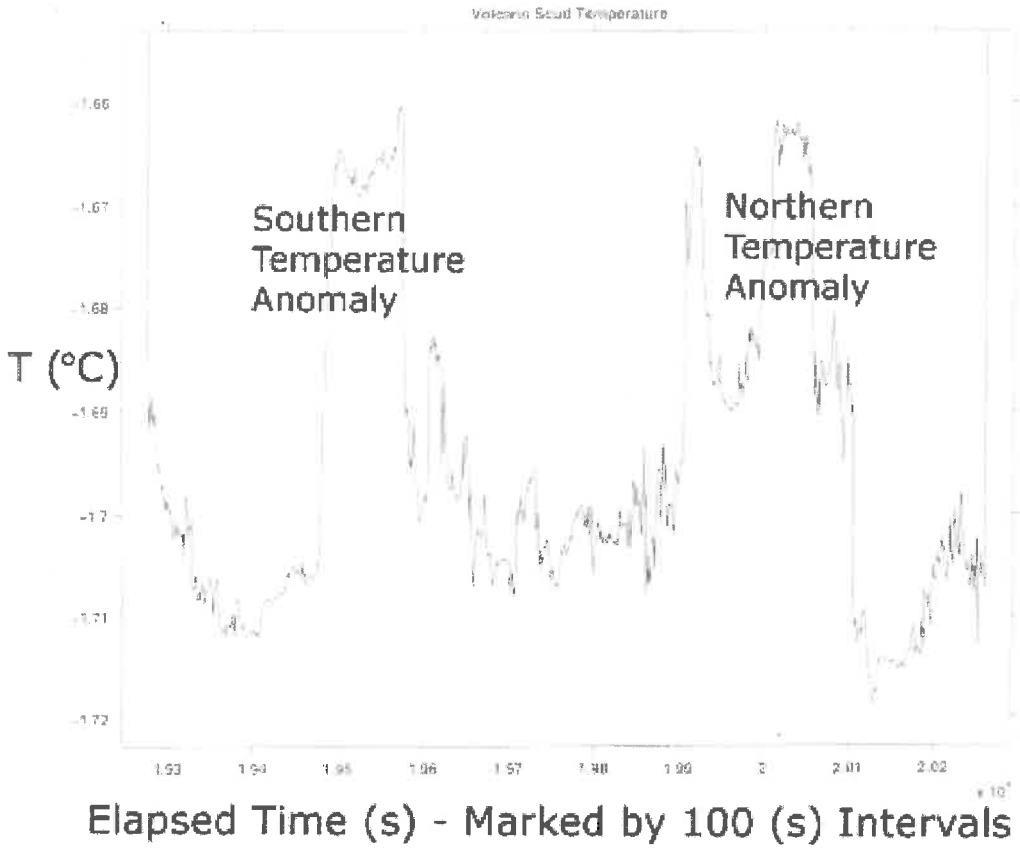

The dredge collected approximately 13 kg of material, 5 kg of which was volcaniclastic sediment (coarse sand – granule). The dredge also collected 196 larger rock specimens, 80% of which were fresh volcanic rocks while the remainder were glacial IRD. Several palagonites were also collected. The volcanic rocks are highly vesicular, sub-angular, and fine-grained to glassy. The largest volcanic specimen weighed 572.5 g (Hatfield et al., 2004).

CHAPTER 3

Methods

The rock specimens recovered from the dredge were shipped to Hamilton College, Clinton, NY, for systematic analysis. Each sample was thoroughly scrubbed with a sponge and luke-warm tap water to remove any loose particulate or organic matter. Each sample was also submerged in a sonicator for six to eight minutes to further remove excess loose material. The clean specimens were then rinsed individually under reverse-osmosis de-ionized water (RO-H_2O) and laid out to air dry. The clean and dry samples were then weighed individually on a digital mass balance scale, with the exception of the three bags of volcaniclastic sediment, which were weighed by the bag (> 1000 g/bag) (Figure 7).

Figure 7: Histogram of Dredged Sample Weights

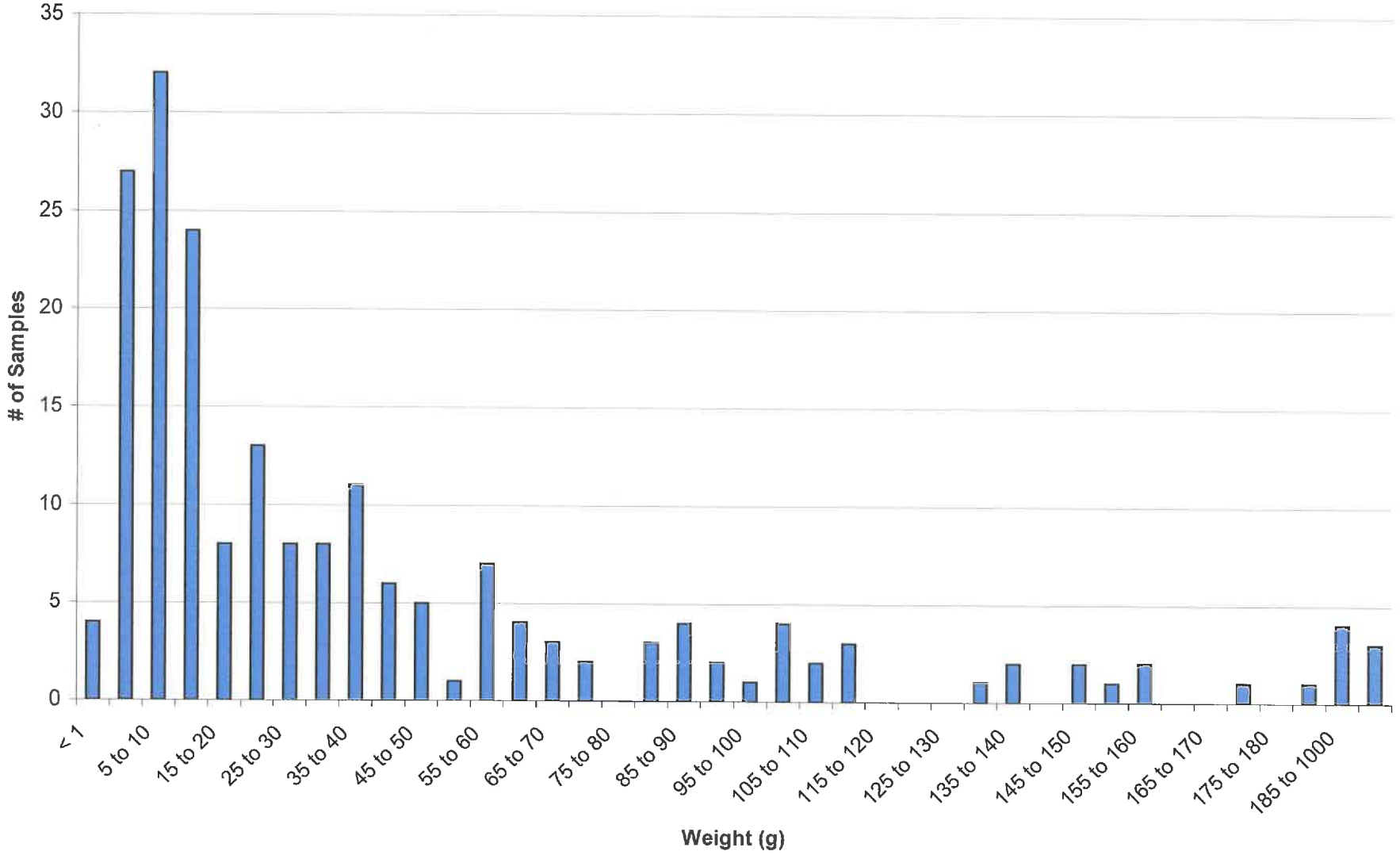

Thirteen representative volcanic samples were selected from the dredge specimens for petrographic and whole-rock chemical analysis (samples JJ04-01 through JJ04-13). A specific account of sample preparation for thin sections is detailed in Appendix B. Whole-rock geochemical data were obtained at Hamilton College by XRF on a Diano automated spectrometer with a duel W/Cr target. A specific account of sample preparation for XRF analysis is detailed in Appendix C. Six of the thirteen samples were further prepared for trace element analysis by ICP-MS at Washington State University (samples JJ04-01, JJ04-04, JJ04-06, JJ04-11, JJ04-12 and JJ04-13). A specific account of sample preparation for ICP-MS is detailed in Appendix D. Samples JJ04-01 and JJ04-06 were also prepared for He-isotope analysis at the University of Rochester. A specific account of sample preparation for He-isotope analysis is detailed in Appendix E.

It was observed that sample JJ04-14 displays a chilled margin, a feature indicative of quick cooling underneath water or ice. Further, three samples (numbered JJ04-20 through JJ04-22) were sent to J. L. Smellie of the British Antarctic Survey.

CHAPTER 4

Petrography

Petrographic observations reveal that olivine, clinopyroxene and plagioclase are present as phenocryst phases. The samples also exhibit a vesicular, sub-trachytic to devitrified glassy groundmass. Several samples also contain small glomerocrysts and xenoliths (Figure 8).

Figure 8: Petrography (Hatfield et al., 2004)

JJ04-01: Olivine-phyric basalt

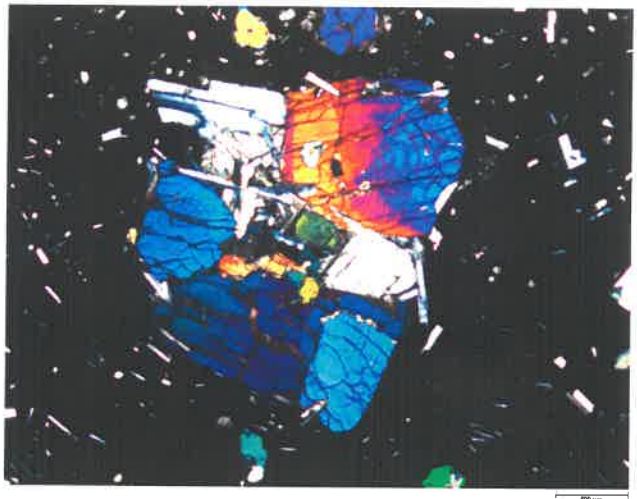

JJ04-02: Clinopyroxene and plagioclase glomeroporphyritic basalt

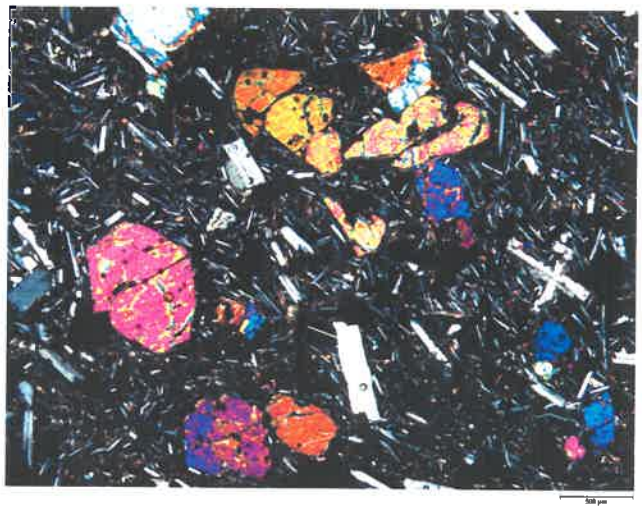

JJ04-06: Olivine and plagioclase-phyric basalt

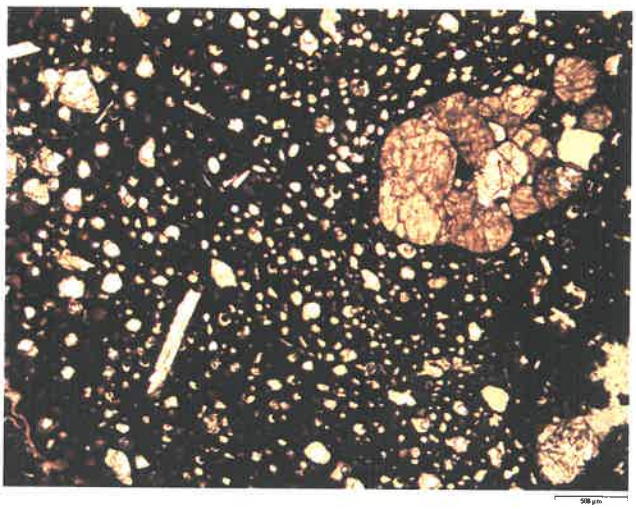

JJ04-09: Vesicular basalt with devitrified glass

CHAPTER 5

Geochemistry

Major, trace, and rare earth element analyses of the Jun Jaegyu alkalic basalts are presented in Appendix A. These data will soon be supplemented by He-isotope data still pending from the University of Rochester. The unpublished chemical data from Jun Jaegyu were compared against published chemical data from previously analyzed volcanic centers in the Antarctic Peninsula.

Major Element Characteristics

According to the IUGS classification diagram for volcanic rocks, the Jun Jaegyu alkalic basalts form a tight grouping of basalts to trachybasalts (< 49 wt. % SiO_2 and 4-6 wt. % $Na_2O + K_2O$). Furthermore, the chemical signature of the Jun Jaegyu alkalic basalts is indistinguishable from volcanic rocks analyzed from the James Ross Island Volcanic Group (Figure 9) (JRIVG data from Smellie, 1990). The two outlying Jun Jaegyu trachybasalt samples (~6 $Na_2O + K_2O$ wt. %) represent two palagonite samples. Thus, the Jun Jaegyu volcanic seamount is both relatively homogenous and chemically similar to other volcanoes in the Antarctic Peninsula region.

Trace Element Characteristics

The range of trace element concentrations for the Jun Jaegyu alkalic basalts relative to average mid-ocean ridge basalt (MORB) of Sun and McDonough (1989) and relative to average primordial mantle of Wood et al. (1979) are shown in figures 10 and 11, respectively. These normalized multi-element diagrams, or spider diagrams, plot an estimate of increasingly incompatible elements in typical mantle from left to right (Winter, 2001). The more incompatible elements graphed on the left-hand side of the diagram should be more enriched in the melt, thus producing a negative slope (Winter, 2001).

Compared to average MORB (Figure 10), the Jun Jaegyu alkalic basalts broadly resemble the trends for ocean island basalts (OIB) and some continental alkali basalts (CAB). The graph reveals Y and Yb concentrations nearly equal to MORB (~1.0), with all the other incompatible elements enriched relative to MORB. However, unlike OIB and CAB, the Jun Jaegyu alkalic basalts do not have a broadly arched pattern that peaks at Ba-Th. Rather, a single peak lies at Th, representing a relative depletion of Ba and Rb. Depletion of Ba and Rb relative to other large ion lithophile elements (LILE) and to the other high field strength elements (HFSE) resembles characteristics of a depleted MORB (Hole, Kempton and Millar, 1993). These findings strongly agree with the findings of Hole, Kempton and Millar (1993) for alkalic basalts analyzed from Alexander Island and The Seal Nunataks.

Figure 10: MORB-normalized multi-element plot: Jun Jaegyu Volcano

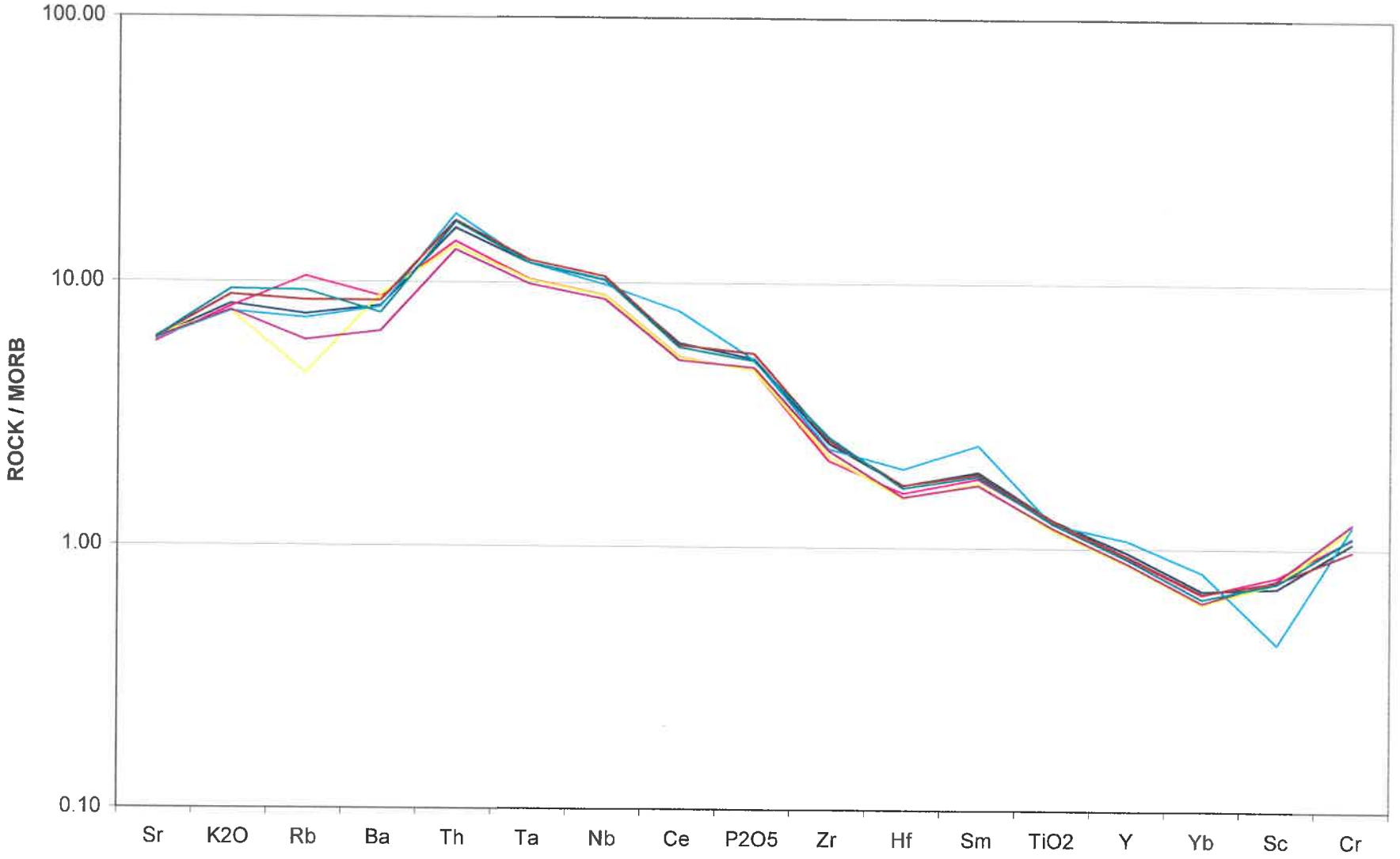

Compared to average primordial mantle (Figure 11), the Jun Jaegyu alkalic basalts again broadly resemble the trends for OIB and CAB. The graph reveals a peak at Nb-Ta and a low at Y. This pattern suggests that Y was compatible during the generation of Jun Jaegyu alkalic basalts, while the other trace elements, such as Nb and Ta, were relatively more incompatible. These findings strongly agree with the findings of Hole et al. (1988) for alkalic basalts analyzed from Alexander Island.

Figure 11: Primordial mantle-normalized multi-element plot: Jun Jaegyu Volcano

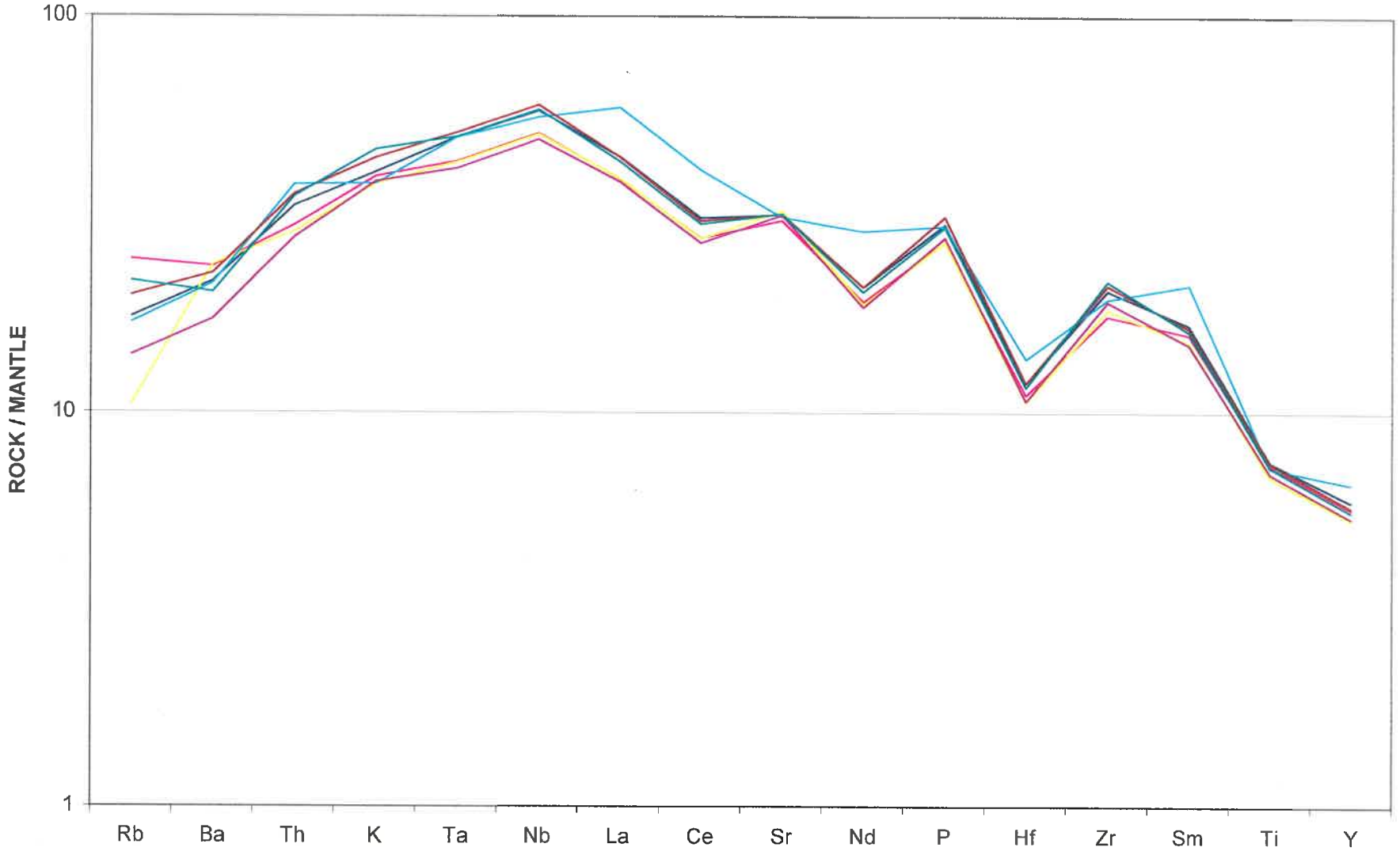

Rare Earth Element Characteristics

The range of rare earth element (REE) concentrations for the Jun Jaegyu alkalic basalts relative to chondrite meteorite concentrations (normalization values obtained from D. Bailey, personal communication) is shown in figure 12. A REE diagram plots an estimate of an increasing degree of compatible elements from left to right (Winter, 2001). A chondrite approximately represents the chemical composition of the early Earth (Winter, 2001). Heavy rare earth elements (HREE) are considered compatible due to their smaller ionic radius (a result of the lanthanide contraction), producing partial melts that are typically HREE depleted (Winter, 2001). HREE are plotted on the right hand side of an REE diagram, resulting in a highly negative slope.

Compared to chondrite (Figure 12) the Jun Jaegyu alkalic basalts exhibit relative LREE enrichment and HREE depletion. This information can be used to infer the depth of origin of the samples because garnet strongly favors HREE (Winter, 2001). The relative depletion of HREE as compared to LREE is consistent with the presence of garnet during partial melting, which occurs at depths over 70 km (Winter, 2001). These findings strongly agree with the findings of Hole et al. (1988) for alkalic basalts analyzed from Alexander Island.

Figure 12: Chondrite-normalized REE plot: Jun Jaegyu Volcano

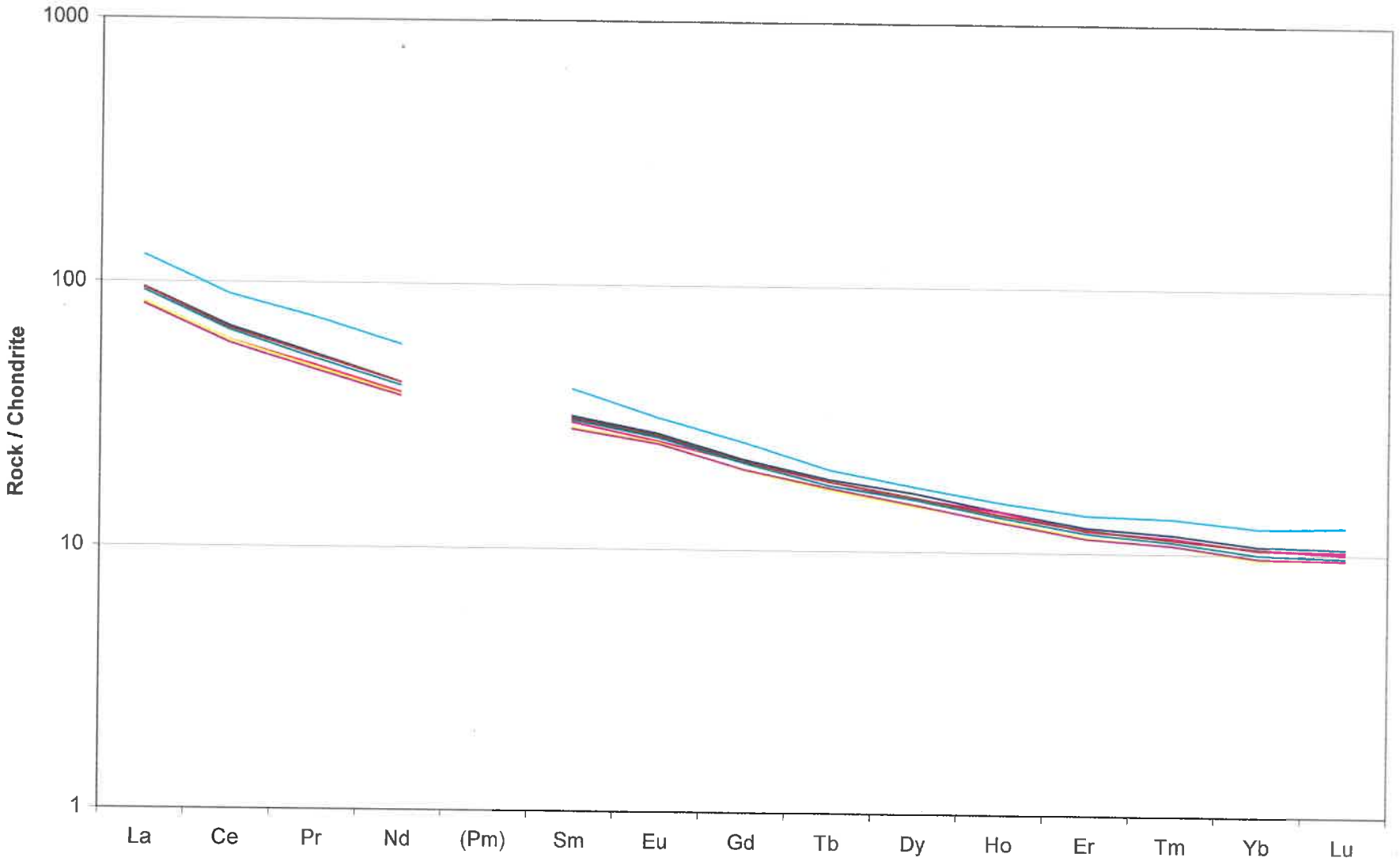

Jun Jaegyu: Plate Margin or Within Plate?

Comparing the average range of trace element concentrations for the Jun Jaegyu alkalic basalts relative to average primordial mantle of Wood et al. (1979) against average values for various plate margin and within-plate volcanic systems reveals interesting trends (Figures 13 and 14, respectively).

The geochemical trends produced from Jun Jaegyu alkalic basalts seem to greatly differ from basalts generated at plate margins (Figure 13). Jun Jaegyu clearly does not resemble the pattern produced by the Andean Arc (Southern Volcanic Zone) (data from Earthchem.org). The Andean Arc exhibits a Ta-Nb trough characteristic of subduction zone magmas (Winter, 2001), whereas Jun Jaegyu shows relative enrichment in Ta-Nb. Also, the Andean Arc (SVZ) exhibits a relative enrichment in Ba as compared to Jun Jaegyu. Both N-MORB (data from Saunders and Tarney, 1984) and P-MORB (Iceland) (data from Schilling et al., 1983 and Earthchem.org) exhibit depleted mantle characteristics, although P-MORB is enriched relative to N-MORB. However, as noted by Hole, Kempton and Millar (1993) the relative depletion in Ba and Rb in Antarctic Peninsula alkali basalts correlates well with the signature of depleted mantle magmas, such as MORB.

Figure 13: Primordial Mantle Normalized Multi-Element Plot: Jun Jaegyu vs. Plate Margin

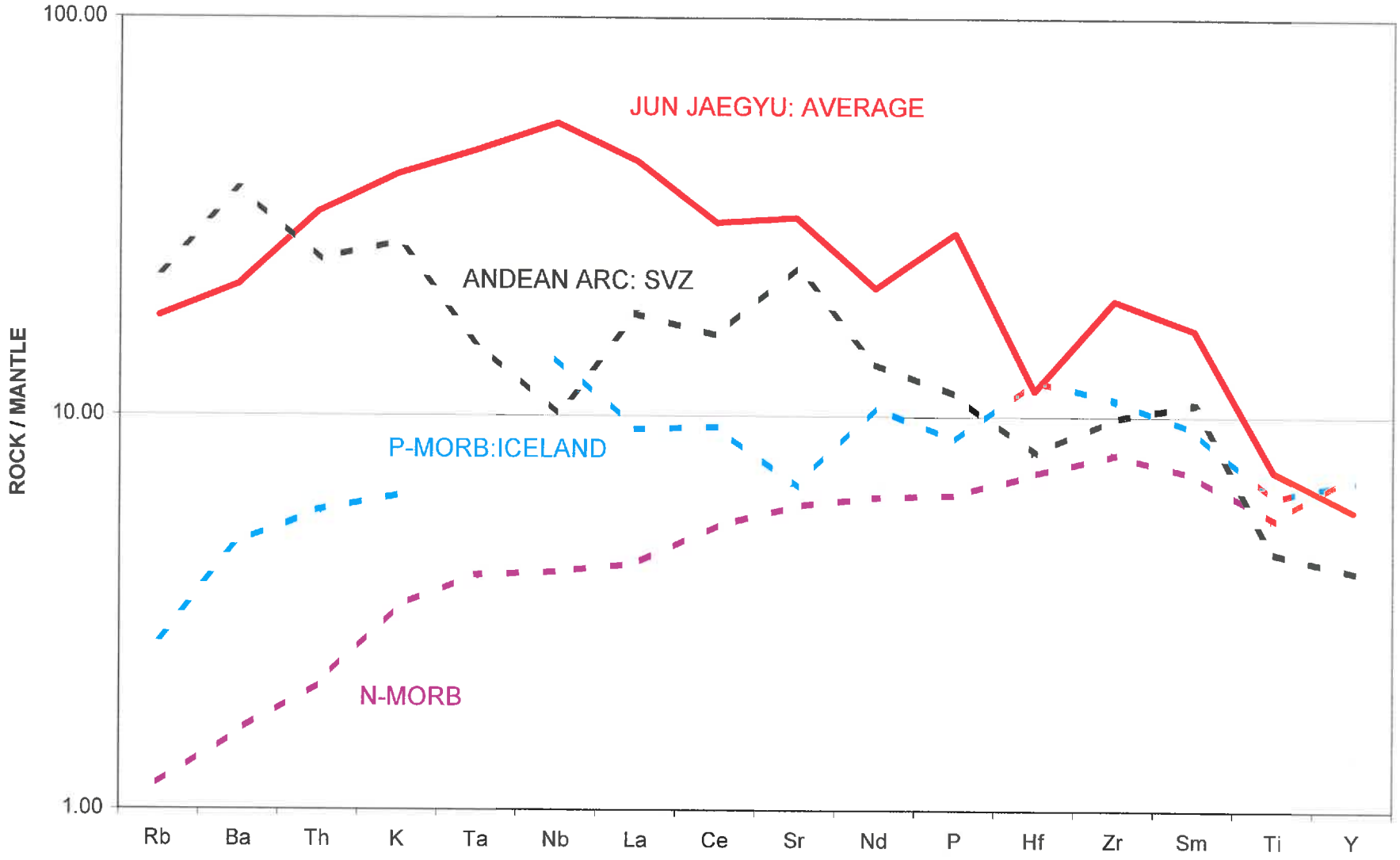

In contrast, the geochemical trends produced from Jun Jaegyu alkalic basalts seem to be broadly consistent with those of within-plate basalts (Figure 14). Jun Jaegyu exhibits characteristics consistent with an asthenospheric origin (Hole, Kempton and Millar, 1993). Samples analyzed from Hawaii and the Columbia River Basalt Group (Hawaii data from the Basaltic Volcanism Study Project, 1981 and Thorpe, 1982; CRBG data from Earthchem.org) exhibit a low at Y similar to Jun Jaegyu. Furthermore, the Hawaii samples also exhibit a relative peak at Nb-Ta, similar to Jun Jaegyu. Interestingly, the Jun Jaegyu alkalic basalts share the greatest likeness with the Hawaii alkalic basalts. Differences arise, however, between the within-plate basalts and Jun Jaegyu alkalic basalts with respect to Jun Jaegyu's relative depletion in Ba and Rb. This depletion is more consistent with the geochemical signature of a depleted MORB (Figure 13). This paradox raises the question of depth of origin for the Jun Jaegyu alkalic basalts: mantle plumes associated with OIB and CAB originate from a depth of at least 650 km, whereas depleted N-MORB originates from 60–80 km depth (Winter, 2001). Previous researchers have argued for multiple melt extraction/depletion episodes affecting small volumes of the upper mantle over the past 1.7 Ga to produce the complex geochemical signatures of the Antarctic Peninsula alkalic basalts (Hole, Kempton and Millar, 1993).

Figure 14: Primordial Mantle Normalized Multi-Element Plot: Jun Jaegyu vs. Within Plate

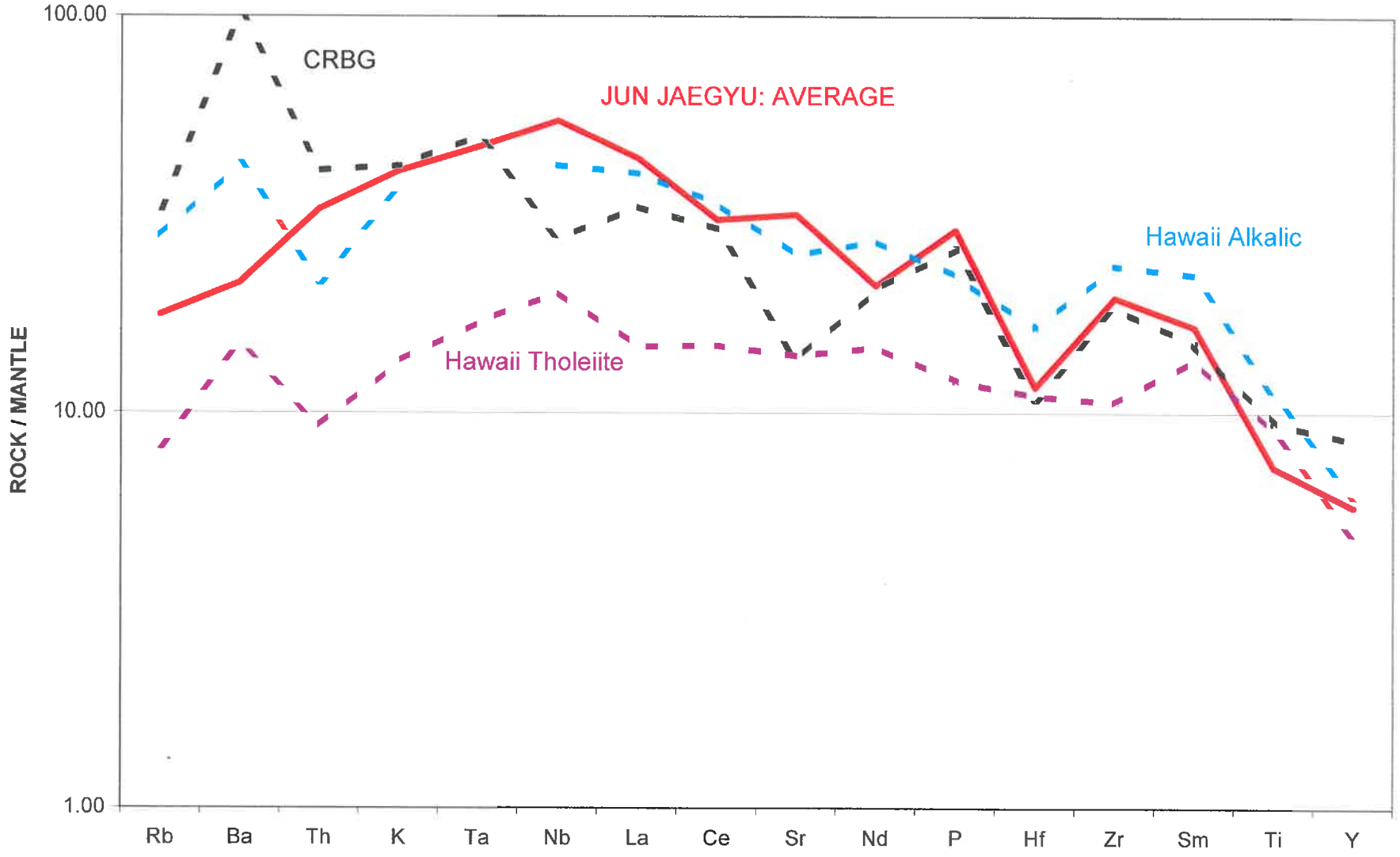

He-Isotopes

In an effort to resolve the question of depth of origin of the asthenospheric source for the Jun Jaegyu alkalic basalts, two samples were prepared for He-isotope analysis. Isotopes of rare gases, such as helium, serve as good petrogenetic indicators for primordial mantle components because ^{3}He is mostly primordial, whereas ^{4}He is mostly radiogenic (Wilson, 1989). ^{4}He is generated by the radioactive decay of ^{232}Th, ^{235}U, and ^{238}U (Wilson, 1989). Variations in $^{3}He/^{4}He$ in volcanic rocks derive from the balance between primordial He and radiogenic He (Wilson, 1989). The ratio is typically normalized to the atmospheric value of $^{3}He/^{4}He$. This normalized He-isotope value ranges from 1-32 in OIB, whereas the normalized He-isotope value ranges from 5-15 in MORB (Wilson, 1989). Thus, a very high He-isotope ratio may represent involvement of primordial mantle components in the melt, which is reflective of a mantle plume. In contrast, a low He-isotope ratio may represent involvement of recycled source components, or a shallow depth of asthenospheric origin (Wilson, 1989).

Currently, we are still awaiting the He-isotope data from the University of Rochester.

CHAPTER 6

Petrogenetic Model for Antarctic Peninsula Alkaline Basalts

The major, trace, and rare earth element data compiled from Jun Jaegyu volcano raise questions about the depth of generation of the basalts, especially when considered in the context of the complex tectonic setting of the Antarctic Peninsula. In a region dominated by subduction for 200 Ma, it seems logical to expect a remnant geochemical signature of subduction. Interestingly, this is not the case. Instead, Jun Jaegyu alkalic basalts show a greater affinity towards within-plate volcanic systems such as OIB and CAB. The other analyzed alkali volcanoes of the Antarctic Peninsula, such as Alexander Island, James Ross Island and The Seal Nunataks, exhibit geochemical trends similar to those of Jun Jaegyu volcano.

Hole, Kempton and Millar (1993) attributed the complex geochemical signature of Antarctic Peninsula alkali volcanic rocks to the generation of small-degree melts of the asthenosphere that did not undergo integration with higher-degree melts, such as occurs at mid-ocean ridges. Further, these small-degree melts of the asthenosphere did not mix with plume-related mantle sources. Instead, this model assumes the low degree partial melting of a garnet lherzolite source (Hole et al., 1988).

This petrogenetic interpretation explains many of the geochemical trends exhibited by alkali basalts analyzed from Alexander Island and The Seal Nunataks, such as:

1) Observed negative Nb-Y correlations and LREE-enrichment (Hole et al., 1988).
2) Relative depletion of Ba and Rb, as well as high K/Rb and K/Ba ratios (Hole, Kempton and Millar, 1993).

Hole, Kempton and Millar (1993) also analyzed several Antarctic Peninsula alkali basalts for isotope variations and concluded the following: Interestingly, a negative ratio of $^{207}Pb/^{204}Pb$ vs. $^{143}Nd/^{144}Nd$ may suggest an ancient depletion event similar to that which produced MORB. Also, the samples analyzed with the lowest $^{87}Sr/^{86}Sr$ ratios have the highest $^{206}Pb/^{204}Pb$ ratios signifying a more recent depletion event that caused an increase in U/Pb ratios, but did not alter Rb/Sr, $^{87}Sr/^{86}Sr$ and $^{143}Nd/^{144}Nd$ ratios. The negative correlation between Nb/Y ratios suggests that relatively high U/Th and U/Pb domains in the mantle were only sampled by the smallest-degree partial melts. Furthermore, the recent increase in U/Pb ratios is not likely a result of metasomatism because of observed low ratios of unradiogenic Sr and LILE/HFSE. Thus, a petrogenetic model depicting a series of melt extraction/depletion episodes that caused depletion in all incompatible trace elements, particularly Ba and Rb, and resulting in high K/Rb and K/Ba ratios, may effectively explain the petrogenetic history of the Antarctic Peninsula alkali basalts.

However, one cannot entirely exclude the possibility of a plume source component without first using a petrogenetic indicator, such as He-isotopes, to ensure the lack of a primordial mantle signature. The data forthcoming from the University of Rochester may prove extremely insightful for the depth of generation for the Antarctic Peninsula alkali basalts.

CHAPTER 7

Conclusions

1) The discovery of Jun Jaegyu volcano adds to the growing number of recognized alkali basalt volcanoes in the Antarctic Peninsula.
2) Jun Jaegyu volcano lies north of the mapped boundary of Cenozoic volcanic rocks in the Antarctic Peninsula, and shows signs indicative of recent activity.
3) Petrographic analysis reveals that olivine, clinopyroxene and plagioclase are present as phenocryst phases.
4) Geochemical analysis reveals that Jun Jaegyu volcano exhibits major, trace, and rare earth element trends consistent with alkali basalts previously analyzed from James Ross Island, Alexander Island and The Seal Nunataks.
5) Geochemically, Jun Jaegyu alkali basalts are most similar to within-plate basalts, particularly OIB and CAB, with the exception of the relative depletion of Ba and Rb.
6) He-isotope analysis forthcoming from The University of Rochester may provide valuable insight pertaining to the depth of the asthenospheric source region of Antarctic Peninsula alkali basalts. High $^{3}He/^{4}He$ ratios would be indicative of a primordial mantle source component (and therefore necessitating a revision of the current petrogenetic model), whereas low $^{3}He/^{4}He$ ratios could be considered as evidence to support the current model proposed by Hole, Kempton and Millar (1993).

REFERENCES

Hatfield, A., Bailey, D., Domack E., Brachfeld, S., Gilbert, R., Ishman, S., Krahmann, G., Leventer, A., (2004), Jun Jaegyu Volcano: A Recently Discovered Alkali Basalt Volcano in Antarctic Sound, Antarctica, *EOS Trans. AGU,* 85(47), Fall Meet. Suppl., Abstract T11A-1248.

Hole, M.J., 1988. Post-subduction alkaline volcanism along the Antarctic Peninsula. *Journal of the Geological Society, London*, 145: 985-998.

Hole, M.J., 1990. Geochemical evolution of Pliocene-Recent post-subduction alkalic basalts from Seal Nunataks Antarctic Peninsula. *Journal of Volcanology and Geothermal Research*, 40: 149-167.

Hole, M.J., Kempton P.D., and Millar I.L., 1993. Trace-element and isotopic characteristics of small-degree melts of the asthenosphere: Evidence from the alkalic basalts of the Antarctic Peninsula. *Chemical Geology*, 109: 51-68.

Hole, M.J. and Larter, R.D., 1993. Trench-Proximal Volcanism Following the Ridge Crest-Trench Collision Along The Antarctic Peninsula. *Tectonics*, 12: 897-910.

Hole, M.J., and LeMasurier W.E., 1994. Tectonic controls on the geochemical composition of Cenozoic mafic alkaline volcanic rocks from West Antarctica. *Contrib Mineral Petrol,* 117: 187-202.

Hole, M.J., Smellie, J.L., and Marriner, G.F. Geochemistry and tectonic setting of Cenozoic alkaline basalts from Alexander Island, Antarctic Peninsula.

LeMasurier, W.E., 1990. Late Cenozoic Volcanism on the Antarctic Plate. Antarctic Research Series, 1-17.

LMG04-04, 2004. Cruise Report. Supported by U.S. National Science Foundation Office of Polar Programs. Obtained by personal communication with E. Domack.

Smellie, J.L., 1987. Geochemistry and Tectonic Setting of Alkaline Volcanic Rocks in the Antarctic Peninsula: A Review. *Journal of Volcanology and Geothermal Research*, 32: 269-285.

Smellie, J.L., 1990. Graham Land and the South Shetland Islands, in LeMasurier et al., ed, Volcanoes of the Antarctic Plate and Southern Oceans; Washington D.C., American Geophysical Union: 303-359.

Wilson, M., 1989. Igneous Petrogenesis – A Global Tectonic Approach. Boston: UNWIN HYMAN, 466 pp.

Winter, J.D., 2001. An Introduction to Igneous and Metamorphic Petrology. New Jersey: Prentice Hall, 697 pp.

FIGURES

Bailey, D., personal communication: chondrite normalization values.

Basaltic Volcanism Study Project, 1981. Basaltic Volcanism on the terrestrial planets. New York: Pergamon Press, 1286 pp.

Earthchem: Advanced Data Management in Solid Earth Geochemistry. Online. 4/27/2005. http://earthchem.org/

GEBCO Atlas. 1997. Antarctic Peninsula Map.

Google.com. 4/30/2005. Images. "Antarctica Map." Online. http://images.google.com/imgres?imgurl=http://www.exportinfo.org/worldfactbook/maps/antarctica_map.gif&imgrefurl=http://www.exportinfo.org/worldfactbook/antarctica_WFB.html&h=377&w=351&sz=35&tbnid=zXdWYYlxkvMJ:&tbnh=118&tbnw=110&hl=en&start=19&prev=/images%3F

Google.com. 4/30/2005. Images. "Antarctica Peninsula Map." Online. http://www.heritage-antarctica.org/ahtuk/images/peninsula1.gif

Saunders, A.D. and J. Tarney, 1984. Geochemical characteristics of basaltic volcanism within back-arc basins. In Marginal basin geology: volcanic and associated sedimentary and tectonic processes in modern and ancient marginal basins, B.P. Kokelaar and M.F. Howells, eds. Geol. Soc. London Spec. Publ., 16: 59-76.

Schilling, J. –G., M. Zajac, R. Evans, T. Johnston, W. White, J.D. Devine, and R. Kingsley, 1983. Petrologic and geochemical variations along the Mid-Atlantic Ridge from 27°N to 73°N. Am. J. Sci. 283: 510-86.

Sun, S. –S. and W.F. McDonough, 1989. Chemical and isotopic systematics of ocean basalts: Implications for mantle composition and processes. In A.D. Saunders and M..J. Norry eds. Magmatism in the Ocean Basins. Geol. Soc. London Spec. Publ., 42: 313-345.

Thorpe, R.S. (ed), 1982. Andesites: orogenic andesites and related rocks. Chickester: Wiley, 697 pp.

Wood, D.A., J.L. Joron, and M. Treuil, 1979. A re-appraisal of the use of trace elements to classify and discriminate between magma series erupted in different tectonic settings. Earth Planet. Sci. Lett., 45: 326-336.

APPENDICES

Appendix A: Geochemical Data

Sample:	JJ04-01	JJ04-02	JJ04-03	JJ04-04	JJ04-05	JJ04-06	JJ04-07	JJ04-08	JJ04-09	JJ04-10
Normalized Major Elements (Weight %):										
SiO_2	47.75	47.41	47.79	47.55	47.63	47.14	48.02	47.85	47.30	46.60
TiO_2	1.92	1.87	1.86	1.89	2.02	1.76	1.82	1.86	1.87	1.71
Al_2O_3	15.24	15.86	15.64	15.43	15.83	16.08	15.49	15.47	15.95	15.64
Fe_2O_3	11.41	10.97	10.95	11.10	11.11	10.87	11.14	11.08	11.06	10.94
MnO	0.16	0.16	0.15	0.16	0.16	0.15	0.15	0.16	0.16	0.15
MgO	8.59	8.83	8.13	8.00	7.47	8.90	8.68	8.41	8.66	9.58
CaO	8.85	9.47	8.94	9.45	7.13	9.12	9.09	9.49	9.16	7.91
Na_2O	3.80	3.33	3.86	3.14	4.85	3.47	3.46	3.46	3.75	4.45
K_2O	1.23	1.20	1.25	1.20	1.69	1.15	1.15	1.15	1.32	1.12
P_2O_5	0.62	0.61	0.58	0.56	0.73	0.56	0.58	0.62	0.65	0.67
TOTAL	99.57	99.72	99.14	98.47	98.62	99.20	99.57	99.52	99.88	98.77
LOI	0.18	3.80	0.62	1.82	9.74	1.01	0.03	-0.13	2.87	9.88
XRF Trace Elements (ppm):										
Sc	26	28	29	28	27	29	30	29	28	25
V	207	199	209	209	205	202	205	203	201	182
Cr	264	300	264	275	195	302	290	305	282	272
Ni	73	108	68	100	22	99	91	97	80	55
Zn	86	107	89	87	87	82	87	85	87	91
Ba	162	152	174	177	204	179	169	160	154	95
Rb	15	12	16	21	28	9	15	15	13	6
Sr	730	755	742	706	707	747	714	719	745	534
Zr	224	214	206	193	233	200	207	213	218	204

ICP-MS Trace Elements (ppm):				
La	31.49	27.71	27.80	41.74
Ce	59.13	52.58	52.44	77.93
Pr	6.61	5.99	5.87	9.06
Nd	26.82	24.60	24.20	37.15
Sm	6.41	6.07	5.80	8.10
Eu	2.13	2.00	1.97	2.44
Gd	6.12	5.97	5.59	7.09
Tb	0.98	0.93	0.89	1.06
Dy	5.73	5.49	5.12	6.05
Ho	1.09	1.09	1.01	1.18
Er	2.82	2.74	2.59	3.14
Tm	0.39	0.38	0.36	0.45
Yb	2.37	2.29	2.10	2.77
Lu	0.36	0.35	0.33	0.43
Ba	205.17	194.67	190.21	775.91
Th	3.21	2.86	2.75	3.62
Nb	35.84	31.47	31.29	34.47
Y	29.07	27.91	26.20	32.25
Hf	4.15	3.88	3.72	4.78
Ta	2.13	1.86	1.84	2.12
U	1.03	0.91	0.89	1.02
Pb	4.16	4.30	3.75	9.43
Rb	18.88	17.89	13.65	115.62
Cs	0.55	0.57	0.26	0.63
Sr	745.84	721.45	794.03	1165.81
Sc	28.42	31.42	29.83	17.44
Zr	190.48	172.72	169.79	164.20

Appendix A: Geochemical Data

JJ04-11	JJ04-12	JJ04-13
Normalized Major Element		
47.71	48.01	48.58
1.80	1.91	1.87
15.74	16.05	16.08
11.11	10.66	10.76
0.16	0.16	0.15
9.42	7.97	8.73
9.41	9.34	9.04
3.32	3.63	3.76
1.17	1.34	1.40
0.58	0.65	0.61
100.39	99.69	100.96
1.47	0.34	0.87
XRF Trace Elements (ppm)		
29	27	28
204	199	192
313	246	278
113	85	84
87	91	86
130	170	152
12	17	19
729	732	733
210	231	237
ICP-MS Trace Elements (pp		
27.26	31.43	30.58
51.14	58.19	57.05
5.76	6.54	6.34
23.80	26.82	26.02
5.73	6.30	6.18
1.95	2.10	2.06
5.61	6.02	5.93
0.91	0.96	0.93
5.19	5.52	5.42
0.99	1.06	1.04
2.56	2.77	2.69
0.36	0.37	0.37
2.13	2.31	2.20
0.33	0.34	0.33
186.40	215.84	211.27
2.66	3.43	3.38
30.36	37.03	36.04
26.45	28.13	27.47
3.74	4.15	4.05
1.78	2.19	2.13
0.88	1.12	1.08
3.98	4.72	4.83
12.18	22.23	19.59
0.33	0.65	0.49
776.88	797.63	794.39
30.63	30.21	29.72
167.55	187.80	184.49

Appendix B

Thin Section Preparation

-Samples JJ04-01 through JJ04-13 were cut into 1x1.5" billets on a 10" diamond rock saw.

-Rinsed and cleaned each cut billet in the sonicator. Each sample individually rinsed with RO-H_2O.

-Dried and warmed the clean billets on a hot plate for 1.5 hours at 125°C. Allowed billets to cool and applied a thin layer of Hillquist impregnating epoxy to the surface of each sample. Allowed epoxy to seep into each rock for ten minutes and then applied another coat of impregnating epoxy. Warmed impregnated billets on a hot plate for one hour at 175°C, and then allowed billets to cool.

-Billets were polished on 12x12x1/4" square glass plates with increasingly finer grades (#80, #220, #400, #800, and #1200) of SiC microgrit. Samples were sonicated in-between each grade of microgrit.

-Polished billets were dried and warmed on a hot plate for one hour at 125°C, and then allowed to cool.

-Thin section glass and polished billets were cleaned with isopropyl alcohol.

-Cleaned, polished billets were glued to clean thin section slides with Hillquist thin section epoxy and were heat-cured on a hot plate for one hour at 75°C. Thin sections continued to cure at room temperature for 24 hours.

-Excess rock was cut and polished off of thin sections with the Hillquist thin section machine.

-Thin sections were polished again on 12x12x1/4" square glass plates with increasingly finer grades (#400 #800 and #1200) of SiC microgrit until they reached 30 μm thickness. Samples were sonicated in-between each grade of microgrit.

-Each thin section was labeled with a diamond tip electric engraver.

-A drop of baby oil and a cover slip were added to improve optical quality of the thin sections.

Appendix C

XRF Fused Glass Bead Preparation

-Samples JJ04-01 through JJ04-13 were wrapped in newspaper and broken apart with a large sledgehammer (newspaper was used to contain the rock fragments).

-The rock fragments were chipped into smaller pieces by hand with a metal mortar and pestle.

-The rock chips from each sample were separately placed in a glass beaker and rinsed in tap water, then sonicated for three minutes, then again rinsed in tap water and finally rinsed in dH_2O.

-The clean chips from each sample were air dried.

-Clean, dry chips were powdered in the SPEX 8510 Shatterbox in a tungsten carbide (WC) dish for 1 ½ minutes.

-The tungsten carbide dish was thoroughly cleaned with compressed air and isopropyl alcohol in-between each sample.

-2g of powdered samples were weighed into quartz crucibles and ignited in Fisher Scientific Isotemp Furnace for 8 hours at 925°C to determine LOI wt. % (Appendix A).

-Ignited powders were mixed in a ceramic mortar and pestle in a 5:1 flux:rock ratio with ultra pure, fused, anhydrous lithium borates-lithium bromide flux. The mortar and pestle were cleaned with isopropyl alcohol in-between samples.

- The flux:rock mixture was transferred to platinum (Pt) crucibles and fused in the Claisse BIS Fluxer for 16 minutes at >1000°C.

-The resulting fused glass beads were labeled and stored in a desiccator.

-Glass beads were cleaned in isopropyl alcohol prior to XRF analysis.

Appendix D

ICP-MS Sample Preparation

-The chips from six samples, JJ04-01, JJ04-04, JJ04-06, JJ04-11, JJ04-12, and JJ04-13, were powdered in the SPEX 8510 Shatterbox in an alumina (Al_2O_3) dish for 4 minutes.

-The aluminum dish was thoroughly cleaned with compressed air and isopropyl alcohol in-between each sample.

-Powdered samples were mixed in a ceramic mortar and pestle in a 1:1 flux:rock ratio with anhydrous lithium tetraborate flux. The mortar and pestle were cleaned with isopropyl alcohol in-between samples.

- The flux:rock mixture was transferred to graphite (C) crucibles and melted in the Fisher Scientific Isotemp Furnace for 1 hour at 950°C.

-The melted samples were removed from the furnace and quickly cooled to room temperature.

-Cooled beads were cleaned with a kim-wipe and then powdered in the SPEX 8510 Shatterbox in an alumina (Al_2O_3) dish for 1 minute.

-The alumina dish was thoroughly cleaned with compressed air and isopropyl alcohol in-between each sample.

-A blank sample of lithium tetraborate was prepared as well. 4.0000 g of Li-Tet was fused and powdered in the same manner as the samples.

-Completed powders were stored in labeled plastic vials and shipped to WSU for analysis.

Appendix E

He Isotope Sample Preparation

-Samples JJ04-01 and JJ04-06 were each wrapped individually in newspaper and crushed with a sledgehammer (the newspaper served to contain all loose rock fragments).

-Chipped pieces of each sample were further crushed in a ceramic mortar and pestle.

-Each crushed rock individually scrutinized under a reflected light microscope for olivine crystals.

-Olivine crystals individually picked out with tweezers and stored in two separate small plastic Petri dishes.

-0.300 g of olivine from each sample shipped to the University of Rochester for analysis.